Hierarchical Economic Optimization of Oil Production from Petroleum Reservoirs

Gijs M. van Essen * **Paul M.J. Van den Hof** *
Jan Dirk Jansen **

* *Delft Center for Systems & Control, Delft University of Technology, Mekelweg 2, 2628 CD Delft, the Netherlands, (e-mail: g.m.vanessen@tudelft.nl, p.m.j.vandenhof@tudelft.nl).*
** *Department of Geotechnology, Delft University of Technology, Stevinweg 1, 2628 CN Delft, the Netherlands / Shell International E&P, Kesslerpark 1 ,2288 GS Rijswijk, the Netherlands (e-mail: jan-dirk.jansen@shell.com).*

Abstract: In oil production *waterflooding* is a popular recovery technology, which involves the injection of water into an oil reservoir. Studies on model-based dynamic optimization of waterflooding strategies have demonstrated that there is a significant potential to increase life-cycle performance, measured in Net Present Value. However, in these studies the complementary desire of oil companies to maximize daily production is generally neglected. To resolve this, a hierarchical optimization structure is proposed that regards economic life-cycle performance as primary objective and daily production as secondary objective. The existence of redundant degrees of freedom allows for the optimization of the secondary objective without compromising optimality of the primary objective.

Keywords: Optimal control, hierarchical structures, redundant DOF, numerical simulation, oil recovery, waterflooding.

1. INTRODUCTION

Oil is produced from subsurface reservoirs. In these reservoirs the oil is contained in the interconnected pores of the reservoir rock under high pressure and temperature. The depletion process of a reservoir generally consists of two production stages. In the primary production stage the reservoir pressure is the driving mechanism for the production. During this phase, the reservoir pressure drops and production gradually decreases. In the secondary production stage liquid (or gas) is injected into the reservoir using injection wells. The most common secondary recovery mechanism involves the injection of water and is referred to as *waterflooding*. It serves two purposes: sustaining reservoir pressure and sweeping the oil out of pores of the reservoir rock and replacing it by water.

Due to heterogeneity of the reservoir rock, the flowing fluids do not experience the same resistance at different points and in different directions in the reservoir. As a result, the oil-water front may not move uniformly towards the production wells, but has a rather irregular shape as depicted schematically in Figure 1. Due to this phenomenon - referred to as *fingering* - the oil-water front may reach the production wells while certain parts of the reservoir are not be properly drained. The produced water must be disposed of in an environmentally friendly way, bringing along additional production costs. At some point the production is no longer economically viable and the wells are closed (shut-in). At the end of the life of the reservoir all production wells are shut-in, while large amounts of oil may still be present in the reservoir.

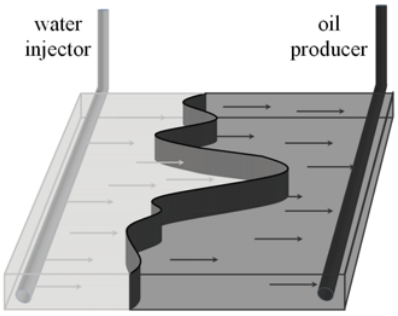

Fig. 1. *Process of waterflooding using a (horizontal) injection and production well. The irregular-shaped oil-water front is a result of the heterogeneous nature of the reservoir, after Brouwer and Jansen (2004).*

Although the injection and production rates of the wells can be manipulated dynamically, they are generally held constant at the maximum capacity of the wells until they are shut-in. Replacing this reactive waterflooding strategy by a dynamic, more proactive one can vastly improve sweep efficiency. Different optimization studies have demonstrated using a numerical reservoir model that there is a potential increase possible of up to 15%, see Brouwer and Jansen (2004) and Jansen et al. (2008). In these optimization studies the objective function is usually of an economic type, most often Net Present Value (NPV), evaluated over the life of the reservoir.

Although many oil companies acknowledge the need for improving economic efficiency over the entire life of the

waterflooding project, many of them adopt maximizing daily production as objective, due to the uncertainty in future economic circumstances. These two objectives, the long-term (life-cycle) objective and the short-term (daily) objective, lead to different, generally conflicting waterflooding strategies.

The goal of this paper is to address the problem of multiple objectives in the optimization of oil recovery from a petroleum reservoir. To that end, a hierarchical optimization structure is proposed that requires a prioritization of the objectives.

This paper proceeds as follows. In Section 2 the properties and characteristics of the reservoir model are described. In Section 3 the life-cycle optimization problem is presented and a hierarchical optimization procedure is proposed. Section 4 deals with identifying redundant degrees of freedom in the optimization problem. The hierarchical optimization procedure is applied to a 3D reservoir model in Section 5. Finally, in Section 6 the results are discussed and alternative approaches are proposed.

2. RESERVOIR MODELING

Reservoir simulators use conservation of mass and momentum equations to describe the flow of oil, water or gas through the reservoir rock. For simplicity reasons, in the oil reservoirs models used within this work only the oil and water phase are assumed to be present.

The mass balance is expressed as follows:

$$\nabla\left(\rho_i u_i\right) + \frac{\partial}{\partial t}\left(\phi \rho_i S_i\right) = 0, \quad i = o, w, \tag{1}$$

where t is time, ∇ the divergence operator, ϕ is the porosity (volume fraction of void space), ρ_i is the density of the phase i, u_i the superficial velocity and S_i the saturation, defined as the proportion of the pore space occupied by phase i.

Conservation of momentum is governed by the Navier-Stokes equations, but is normally simplified for low velocity flow through porous materials, to be described by the semi-empirical Darcy's equation as follows:

$$u_i = -k\frac{k_{ri}}{\mu_i}\nabla p_i, \quad i = o, w, \tag{2}$$

where p_i is the pressure of phase i, k is the absolute permeability, k_{ri} is the relative permeability and μ_i is the viscosity of phase i. The permeability k is an inverse measure of the resistance a fluid experiences flowing through the porous medium. The relative permeability k_{ri} relates to the additional resistance phase i experiences when other phases are present, due to differences in viscosity. As a result, it is a strongly non-linear function of the saturation S_i. In (2) gravity is discarded for simplicity reasons. However, within the 3D example presented in this paper, gravity does play a role. For a more complete description of Darcy's equation we refer to literature, see Aziz and Settari (1979).

Substituting (2) into (1) results into 2 flow equations with 4 unknowns, p_o, p_w, S_o and S_w. Two additional equations are required to complete the system description. The first is the closure equation requiring that the sum of phase saturations must equal 1:

$$S_o + S_w = 1 \tag{3}$$

Second, the relation between the individual phase pressures is given by the capillary pressure equation:

$$p_{cow}(S_w) = p_o - p_w \tag{4}$$

Common practice in reservoir simulation is to substitute (3) and (4) into the flow equations, by taking the oil pressure p_o and water saturation S_w as primary state variables:

$$\nabla(\tilde{\lambda}_o \nabla p_o) = \frac{\partial}{\partial t}\left(\phi\rho_o \cdot [1 - S_w]\right), \tag{5}$$

$$\nabla\left(\tilde{\lambda}_w \nabla p_o - \tilde{\lambda}_w \frac{\partial p_{cow}}{\partial S_w}\nabla S_w\right) = \frac{\partial}{\partial t}\left(\phi\rho_w S_w\right), \tag{6}$$

where $\tilde{\lambda}_o = k\frac{k_{ro}}{\mu_o}$ and $\tilde{\lambda}_w = k\frac{k_{rw}}{\mu_w}$ are the oil and water mobilities. Flow equations (5) and (6) are defined over the entire volume of the reservoir. It is assumed that there is no flow across the boundaries of the reservoir geometry over which (5)-(6) is defined (Neumann boundary conditions).

Due to the complex nature of oil reservoirs, (5)-(6) generally cannot be solved analytically, hence they are evaluated numerically. To this purpose the equations are discretized in space and time. The discretization in space leads to a system built up of a finite number of blocks, referred to as *grid blocks*. This results in the following state space form:

$$\mathbf{V}(\mathbf{x}_k)\cdot\mathbf{x}_{k+1} = \mathbf{T}(\mathbf{x}_k)\cdot\mathbf{x}_k + \mathbf{q}_k, \quad \mathbf{x}_0 = \bar{\mathbf{x}}_0, \tag{7}$$

where k is the time index and $\mathbf{x}$ is the state vector containing the oil pressures (p_o) and water saturations (S_w) in all grid blocks. Vector $\bar{\mathbf{x}}_0$ contains the initial conditions, which are assumed to be known. In the discretization of (5)-(6), the units are converted from $[\frac{kg}{m^3 s}]$ to $[\frac{m^3}{s}]$. In (7) a source vector $\mathbf{q}_k$ is added to model the influence of the wells on the dynamic behavior of the reservoir. The source terms are usually represented by a so-called well model, which relates the source term to the pressure difference between the well and grid block pressure:

$$q_k^j = w^j \cdot (p_{bh,\,k}^j - p_k^j), \tag{8}$$

where $p_{bh,\,k}$ is the well's bottom hole pressure, j the index of the grid block containing the well and p_k^j the grid block pressure in which the well is located. The term w is a well constant which contains the well's geometric factors and the rock and fluid properties of the reservoir directly around the well.

The geological properties inside each grid block are assumed to be constant. The strongly heterogeneous nature of the reservoir can be characterized by assigning different property values to each of the grid blocks. Usually a very large number of grid-blocks is required ($10^3 - 10^6$) to adequately describe the fluid dynamics of a real petroleum reservoir.

The reservoir simulations used within this study are performed using the reservoir simulation software package MoReS, which has been developed by Shell.

3. WATERFLOODING OPTIMIZATION PROBLEM

Flooding a reservoir with water to increase oil production is essentially a batch process, with the additional characteristic that there is no repetition involved. Due to the fact that performance is evaluated at the end of the process and the time constants associated with the nonlinear dynamics are very long, a receding horizon approach will most likely not result in optimal depletion of a reservoir. Dynamic optimization over the entire life of the reservoir is required which can be expressed by the following mathematical formulation:

$$\max_{\mathbf{u}} J(\mathbf{u}), \tag{9}$$

$$s.t.\ \mathbf{x}_{k+1} = \mathbf{f}\left(\mathbf{x}_k, \mathbf{u}_k\right),\ k = 1, .., K, \quad \mathbf{x}_0 = \bar{\mathbf{x}}_0, \tag{10}$$

$$\mathbf{g}(\mathbf{u}) \leq 0 \tag{11}$$

where $\mathbf{u}$ is the input trajectory, $\mathbf{f}$ represents the system equations as described in (7) and $\bar{\mathbf{x}}_0$ is a vector containing the initial conditions of the reservoir. The inequality constraints $\mathbf{g}(\mathbf{u})$ relate to the capacity limitations of the wells.

The objective function J is of an economic type, generally Net Present Value:

$$J = \sum_{k=1}^{K} \left[\frac{r_o \cdot q_{o,k} - r_w \cdot q_{w,k} - r_{inj} \cdot q_{inj,k}}{(1+b)^{\frac{t_k}{\tau_t}}} \cdot \Delta t_k \right], \tag{12}$$

where r_o is the oil revenue $[\frac{\$}{m^3}]$, r_w the water production costs $[\frac{\$}{m^3}]$ and r_{inj} the water injection costs $[\frac{\$}{m^3}]$, which are all assumed constant. K represents the total number of time steps k of a fixed time span and Δt_k the time interval of time step k in $[day]$. The term b represents the discount rate for a certain reference time τ_t. The terms $q_{o,k}$, $q_{w,k}$ and $q_{inj,k}$ represent the total flow rate of respectively produced oil, produced water and injected water at time step k in $[\frac{m^3}{day}]$. An economic objective functions like (12) does not necessarily provide a unique solution to the optimization problem. Although it relates to realistic business conditions, it may well cause ill-posedness of the problem.

Several methods are available for dynamic optimization of large scale problems, see Bryson (1999), Schlegel et al. (2005) and Biegler (2007). *Simultaneous* methods have attractive convergence and constraint handling properties, but even though their capacity to cope with large-scale problems has increased considerably over the recent years, models of order 10^6 still remain very difficult to handle. Although *sequential* methods require repeated numerical integration of the model equations, only the control vector is parameterized and as a result can deal with larger problems. Secondly, due to the fact that the flooding process is very slow much time is available to perform the usually large number of required simulations. However, if the number of control parameters grows the required simulation time may still become unfeasible at some point, unless a method is available to efficiently calculate the gradients of the objective function with respect to the control parameters. This can be done by integration of the adjoint equations or directly through sensitivity equations of model equations.

In the reservoir simulation package used within this work, the adjoint equations are implemented to calculate the gradients. For simplicity reasons, a Steepest Ascent (SA) algorithm is adopted to determine improving control parameters.

3.1 Hierarchical optimization

In the life-cycle waterflooding problem as expressed by (9)-(11), the desire of many oil companies to maximize short-term (daily) production is discarded. A balanced objective provides a possibility to address both objectives in a single function. However, finding an suitable weighting between the objectives may prove to be difficult. Alternatively, we propose a hierarchical (or lexicographic) optimization structure that requires a prioritization of the multiple objectives, as described in Haimes and Li (1988) and Miettinen (1999). In this structure, optimization of a secondary objective function J_2 is constrained by the requirement of the primary objective function J_1 to remain close to its optimal value J_1^*. This structure can be expressed mathematically as follows:

$$\max_{\mathbf{u}} J_2(\mathbf{u}), \tag{13}$$

$$s.t.\ \mathbf{x}_{k+1} = \mathbf{f}\left(\mathbf{x}_k, \mathbf{u}_k\right),\ k = 1, .., K, \quad \mathbf{x}_0 = \bar{\mathbf{x}}_0 \tag{14}$$

$$\mathbf{g}(\mathbf{u}) \leq 0 \tag{15}$$

$$J_1^* - J_1(\mathbf{u}, \mathbf{x}) \leq \varepsilon \tag{16}$$

where ε is an arbitrary small value compared to J_1^*. Solving (13) - (16) requires the knowledge of J_1^*, which is obtained through solving optimization problem (9) - (11).

4. REDUNDANT DEGREES OF FREEDOM

In Jansen et al. (2009) it was observed that significantly different optimized waterflooding strategies result in nearly equal values in NPV. They concluded that the flooding optimization problem is ill-posed and contains many more control variables than necessary. This suggests that optimality of an economic life-cycle objective in waterflooding optimization does not fix all degrees of freedom (DOF) of the decision variable space $\mathcal{D}$, i.e. there exist redundant DOF in the optimization problem. Huesman et al. (2008) found similar results for economic dynamic optimization of plant-wide operation.

A consequence of these redundant DOF is that even if ε in (16) is chosen equal to 0, DOF are left to improve the secondary objective function J_2. A straightforward way of investigating this is to imbed (16) as an equality constraint in the adjoint formulation by means of an additional Lagrange multiplier. Unfortunately, the adjoint functionality in MoReS is not yet capable of dealing with (additional) state constraints. Alternatively, unconstrained gradient information can be used to investigate the redundant DOF, as described in the next section.

4.1 Quadratic approximation of the objective function

A solution $\mathbf{u}$ for which no constraints are active is an optimal solution $\mathbf{u}^*$ if and only if the gradients of J with respect to $\mathbf{u}$ are zero, i.e. $\frac{\partial J}{\partial \mathbf{u}} = 0$. As a result, at $\mathbf{u}^*$ the

gradients do not provide any information on possible redundant degrees of freedom under the optimality condition on J.

Second-order derivatives of J with respect to $\mathbf{u}$ are collected in the Hessian matrix $\mathbf{H}$. If $\mathbf{H}$ is negative-definite, the considered solution $\mathbf{u}$ is an optimal solution, but no DOF are left when the optimality condition on J holds. If $\mathbf{H}$ is negative-semidefinite it means that the Hessian does not have full rank. An orthonormal basis $\mathbf{B}$ for the indetermined directions of $\mathbf{H}$ can than be obtained through a singular value decomposition:

$$\mathbf{H} = \mathbf{U} \cdot \mathbf{\Sigma} \cdot \mathbf{V} \tag{17}$$

The orthonormal basis $\mathbf{B}$ consists of those columns of $\mathbf{V}$ that relate to singular values of zero, i.e. $\mathbf{B} = \{\mathbf{v}_i \mid \sigma_i = 0, \quad i = 1, \ldots, N_{\mathbf{u}}\}$, where $N_{\mathbf{u}}$ is the number of parameters that represent the DOF in the input.

Not all orthogonal directions spanned by the columns of $\mathbf{B}$ will be redundant DOF. These directions are redundant DOF, if they are linear and all higher order derivatives are zero as well, which at this point in time is impossible to proof for reservoir models. $\mathbf{B}$ is however a basis for redundant DOF for a quadratic approximation $\hat{J}$ of objective function J. As $\hat{J}$ can be considered to be an acceptable approximation for small deviations from $\mathbf{u}^*$, $\mathbf{B}$ can be regarded as an acceptable basis for the redundant DOF for small deviations from $\mathbf{u}^*$.

Approximate Hessian matrix Unfortunately, no reservoir simulation package is currently capable of calculating second-order derivatives. However, using the gradient information second-order derivatives can be approximated. Within this work a forward-difference scheme is adopted:

$$\frac{\partial^2 J}{\partial u_i \partial u_j} \approx \frac{\nabla J_i(\mathbf{u} + h_j \mathbf{e}_j) - \nabla J_i(\mathbf{u})}{2h_j} + \frac{\nabla J_j(\mathbf{u} + h_i \mathbf{e}_i) - \nabla J_j(\mathbf{u})}{2h_i} \tag{18}$$

Where $\mathbf{e}_i$ is a canonical unit vector, i.e. a vector with a 1 at element i and 0 elsewhere and h_i is the perturbation step size that relates to parameter u_i of $\mathbf{u}$. In total $N_{\mathbf{u}} + 1$ simulations (function evaluations) are required to obtain the approximate Hessian matrix $\hat{\mathbf{H}}$ at a particular optimal solution $\mathbf{u}^*$.

4.2 Hierarchical optimization method

Adopting the approximation of $\mathbf{H}$ as described in Subsection 4.1, the following iterative procedure is proposed to attack the hierarchical optimization problem (13) - (16) with $\varepsilon = 0$:

(1) Find a (single) optimal strategy $\mathbf{u}^*$ to primary objective function J_1 and use $\mathbf{u} = \mathbf{u}^*$ as starting point in the secondary optimization problem.
(2) Approximate the Hessian matrix $\mathbf{H}$ of J_1 with respect to the input variables at (initial input) $\mathbf{u}$ and determine an orthonormal basis $\mathbf{B}$ for the null-space of $\hat{\mathbf{H}}$.
(3) Find the improving gradient direction $\frac{\partial J_2}{\partial \mathbf{u}}$ for the secondary objective function J_2.

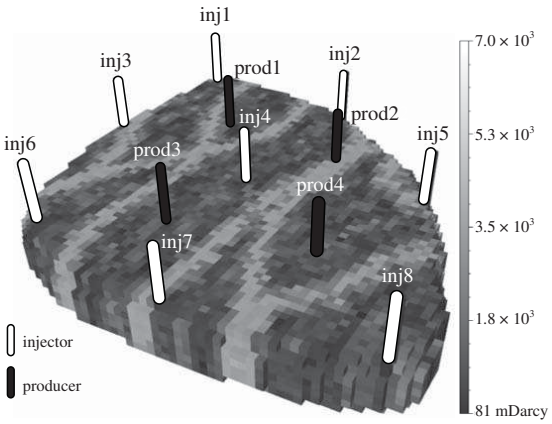

Fig. 2. *3D reservoir model with 4 production and 8 injection wells. The geological structure involves a network of meandering channels in which the fluids flows experience less resistance, due to higher permeability.*

(4) Project $\frac{\partial J_2}{\partial \mathbf{u}}$ onto the orthonormal basis $\mathbf{B}$ to obtain projected direction $\mathbf{d}$, such that $\mathbf{d}$ is an improving direction for J_2, but does not affect J_1. The projection is performed using projection matrix $\mathbf{P}$, see Luenberger (1984):

$$\mathbf{d} = \mathbf{P} \cdot \left(\frac{\partial J_2}{\partial \mathbf{u}} \right)^T \tag{19}$$

$$\mathbf{P} = \mathbf{B} \cdot \left(\mathbf{B} \cdot^T \mathbf{B} \right)^{-1} \cdot \mathbf{B}^T \tag{20}$$

(5) Update $\mathbf{u}$ using projected direction $\mathbf{d}$ in a SA method.

$$\mathbf{u}_{new} = \mathbf{u}_{old} + \tau \cdot \mathbf{d}, \tag{21}$$

where τ is an appropriately small step size such that the quadratic approximation of J_1 is justified.
(6) Perform steps 2 through 6 until convergence of J_2.

In the next section a numerical example is presented where the iterative hierarchical optimization structure is tested on a 3D heterogeneous reservoir model.

5. NUMERICAL EXAMPLE

The hierarchical optimization procedure is applied to a 3-dimensional oil reservoir model, introduced in Van Essen et al. (2006). The life-cycle of the reservoir covers a period of 3,600 days and is chosen such that all oil can be produced within that time frame. The length of the life-cycle is in this example not incorporated as additional optimization parameter. The reservoir model consists of 18,553 grid blocks, as depicted in Figure 2, and has dimensions of $480 \times 480 \times 28$ meter. Its geological structure involves a network of fossilized meandering channels in which the flowing fluids experience less resistance, due to higher permeability. The average reservoir pressure is 400 [*bar*].

The reservoir model contains 8 injection wells and 4 production wells. The production wells are modeled using a well model (8) and operate at a constant bottom hole pressure p_{bh} of 395 [*bar*]. The flow rates of the injection wells can be manipulated directly, i.e. the control input $\mathbf{u}$ involves injection flow rate trajectories for each of the 8

injection wells. The minimum rate for each injection well is 0.0 $[\frac{m^3}{day}]$, the maximum rate is set at a rate of 79.5 $[\frac{m^3}{day}]$.

The control input $\mathbf{u}$ is re-parameterized in time using a zero-order-hold scheme with input parameter vector θ. For each of the 8 injection wells, the control input $\mathbf{u}$ is re-parameterized into 4 time periods t_{θ_i} of 900 days over which the injection rate is held constant at value θ_i. Thus, the input parameter vector θ consists of $8 \times 4 = 32$ elements.

5.1 Life-cycle optimization

The objective function for the life-cycle optimization is defined in terms of NPV, as defined in Equation (12), with $r_o = 126\,[\frac{\$}{m^3}]$, $r_w = 19\,[\frac{\$}{m^3}]$ and $r_i = 6\,[\frac{\$}{m^3}]$. The discount rate b is set to 0. Thus, the life-cycle objective relates to undiscounted cash flow.

The optimal input - denoted by $\mathbf{u}_\theta{}^*$ - obtained after approximately 50 iterations, is shown in Figure 3. None of the input constraints (11) are active for $\mathbf{u}_\theta{}^*$. The value of the objective function corresponding to input $\mathbf{u}_\theta{}^*$ is 47.6×10^6 \$.

5.2 Hierarchical optimization

A secondary objective function J_2 was defined to emphasize the importance of short-term production. To that end, J_2 is chosen identical to the primary objective function but with the addition of a very high annual discount rate b of 0.25. As a result, short-term production is weighed far more heavily than future production. Note that due to the very high discount rate, the actual value of J_2 no longer has a realistic meaning in an economic sense.

The hierarchical approach as presented in Subsection 4.2 is applied. The total number of simulation runs needed to approximate the Hessian ($\hat{\mathbf{H}}$) is 33. However, the required simulation time was vastly reduced by parallel processing the simulations.

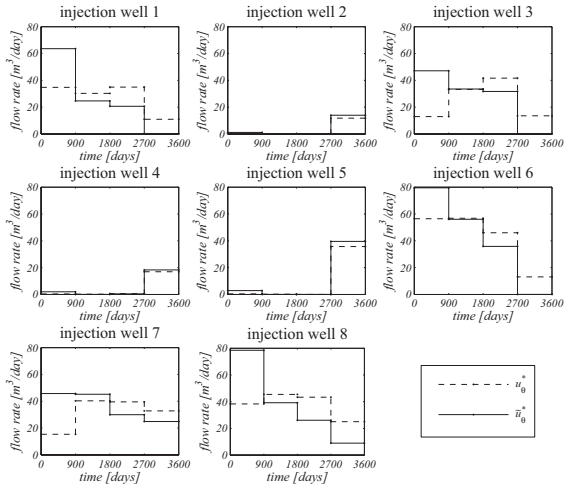

Fig. 3. *Input trajectories for each of the 8 injection wells for the initial optimal solution $\mathbf{u}_\theta{}^*$ to J_1 (dashed line) and the optimal solution $\tilde{\mathbf{u}}_\theta^*$ after the constrained optimization of J_2 (solid line)*

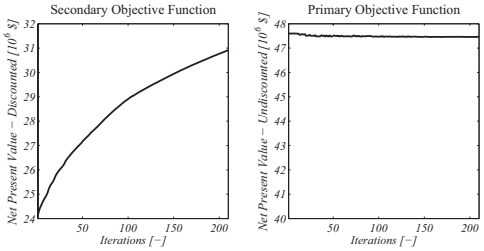

Fig. 4. *Values of the secondary J_2 and primary J_1 objective function plotted against the iteration number for the constrained secondary optimization problem.*

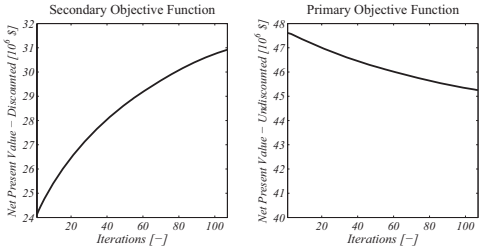

Fig. 5. *Values of the secondary J_2 and primary J_1 objective function plotted against the iteration number for the secondary optimization problem, no longer constrained by the orthonormal basis $\mathbf{B}$.*

Due to the fact that this example involves a numerical model and an approximation of the second-order derivatives, the selection criterion for $\mathbf{B}$ is relaxed. Those columns $\mathbf{v}_i$ of $\mathbf{V}$ were selected that correspond to singular values for which $\frac{\sigma_i}{\sigma_1} < 0.02$ instead of $\sigma_i = 0$. The projected gradients $\mathbf{d}$ were again used in a steepest-ascent scheme. For the quadratic approximation of J_1 to be justified, $\mathbf{u}_{\theta,new}$ must remain close to $\mathbf{u}_{\theta,old}$. To achieve that, $\mathbf{d}$ was normalized and a constant step size τ of 1 was used. Due to time restrictions, the hierarchical optimization of J_2 was terminated after 210 iterations with final control input $\tilde{\mathbf{u}}_\theta^*$. To evaluate the results of the hierarchical optimization, a second optimization case was carried out, where optimization of J_2 was performed *without* projection on $\mathbf{B}$. As a result, the obtained control input - denoted by $\tilde{\mathbf{u}}_\theta$ - does in this case not ensure optimality of J_1.

Figure 4 displays the values of J_1 and J_2 plotted against the iteration number for the hierarchical optimization problem. It shows a considerable increase of J_2 of 28.2% and a slight drop of J_1 of -0.3%. In Figure 3 the input strategy after the final iteration step is presented. It can be observed that the injection strategy shows a substantial increase in injection rates at the beginning of the production life and a decrease at the end. The values of J_1 and J_2 plotted against the iteration number for the *unconstrained* optimization of J_2 are shown in Figure 5. Again an increase of J_2 of 28.2% is realized, but now at a cost of a decrease of J_1 of -5.0%. Finally, Figure 6 shows the value of the primary objective function J_1 over time until the end of the producing reservoir life for $\mathbf{u}_\theta{}^*$, $\tilde{\mathbf{u}}_\theta^*$ and $\tilde{\mathbf{u}}_\theta$. Input $\tilde{\mathbf{u}}_\theta^*$ shows a steeper ascent of J_1 than $\mathbf{u}_\theta{}^*$, while their final values are nearly equal. Input $\tilde{\mathbf{u}}_\theta$ shows initially the same steep ascent as $\tilde{\mathbf{u}}_\theta^*$, but J_1 drops at the end of the life of the reservoir.

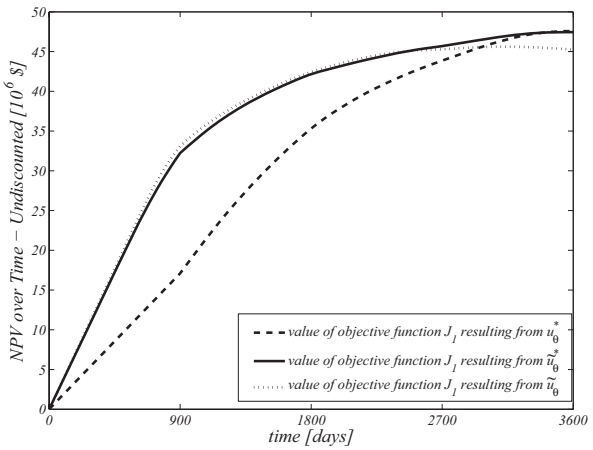

Fig. 6. *Value of the primary objective function J_1 over time for initial optimal input $\mathbf{u}_\theta{}^*$ to J_1 (dashed line), the optimal input $\tilde{\mathbf{u}}_\theta^*$ after the constrained optimization of J_2 (solid line) and input $\tilde{\mathbf{u}}_\theta$ after the unconstrained optimization of J_2 (dotted line)*

6. CONCLUSION

Model-based optimization is a relatively new approach to oil recovery from petroleum reservoirs. Optimization studies have shown a considerable potential increase in life-cycle performance. However, increased understanding of the optimal control problem and characteristics of the optimal solutions is necessary to take the next step towards a real-life application.

Within this work the issue of multiple objectives in oil production is addressed. A hierarchical approach is investigated by means of a simulation experiment. For the presented experiment we conclude that:

- There exist redundant DOF in the input strategy $\mathbf{u}$ with respect to the optimality of the life-cycle objective. This implies the existence of an optimal subset $\mathcal{S}$ of connected optimal solutions within the solution space $\mathcal{D}$.
- The redundant DOF create enough freedom to significantly improve the secondary objective function. Moreover, the difference between the initial and final input strategy to the secondary optimization problem is substantial. This suggest that $\mathcal{S}$ occupies a considerable space within decision variable space $\mathcal{D}$.
- The presented hierarchical optimization procedure provides a method to incorporate short-term performance objectives into problem setting of maximizing life-cycle performance of oil recovery. Using the hierarchical structure, optimization of the secondary objective may be executed without significantly compromising the primary objective.

Under which conditions these conclusions also apply to different life-cycle waterflooding problems and/or different reservoir models will be subject for further investigation.

6.1 Discussion

The presented hierarchical optimization approach is computationally very demanding and becomes infeasible for more realistic reservoir models with an increased number of input parameters. A different method to approximate the Hessian requiring less simulation runs may be considered to resolve this, e.g. the secant method. However, calculating second-order derivatives may be avoided altogether when the hierarchical optimization problem is imbedded in the adjoint formulation, as mentioned in Section 4. This approach will be the focus of future research.

Within this work, uncertainty - of the model and/or the objective function parameters - was neglected. In literature, a number of methods are presented to attack the problem of life-cycle optimization under uncertainty, using a closed-loop approach. For a good overview see Jansen et al. (2008). Without considerable effort, the presented hierarchical optimization structure can be integrated into this closed-loop framework.

REFERENCES

Aziz, K. and Settari, A. (1979). *Petroleum Reservoir Simulation*. Applied Science Publishers.

Biegler, L.T. (2007). An overview of simultaneous strategies for dynamic optimization. *Chemical Engineering and Processing: Process Intensification*, 46(11), 1043–1053. doi:10.1016/j.cep.2006.06.021.

Brouwer, D.R. and Jansen, J.D. (2004). Dynamic optimization of waterflooding with smart wells using optimal control theory. *SPE Journal*, 9(4), 391–402. doi:10.2118/78278-PA. SPE 78278-PA.

Bryson, A.E. (1999). *Dynamic Optimization*. Addison Wesley Longman.

Haimes, Y.Y. and Li, D. (1988). Hierarchical multiobjective analysis for large-scale systems: Review and current status. *Automatica*, 24(1), 53–69. doi:10.1016/0005-1098(88)90007-6.

Huesman, A.E.M., Bosgra, O.H., and Van den Hof, P.M.J. (2008). Integrating mpc and rto in the process industry by economic dynamic lexicographic optimization; an open-loop exploration. In *AIChE Annual Meeting*. Philadelphia, U.S.A.

Jansen, J.D., Bosgra, O.H., and Van den Hof, P.M.J. (2008). Model-based control of multiphase flow in subsurface oil reservoirs. *Journal of Process Control*, 18(9), 846–855. doi:10.1016/j.jprocont.2008.06.011.

Jansen, J.D., Douma, S.D., Brouwer, D.R., Van den Hof, P.M.J., Bosgra, O.H., and Heemink, A.W. (2009). Closed loop reservoir management. In *SPE Reservoir Simulation Symposium*. The Woodlands, Texas, U.S.A. doi:10.2118/119098-MS. SPE 119098-MS.

Luenberger, D.G. (1984). *Linear and nonlinear programming*. Addison-Wesley.

Miettinen, K.M. (1999). *Nonlinear Multiobjective Optimization*. Kluwer Academic Publishers, Boston.

Schlegel, M., Stockmann, K., Binder, T., and Marquardt, W. (2005). Dynamic optimization using adaptive control vector parameterization. *Computers & Chemical Engineering*, 29(8), 1731–1751. doi:10.1016/j.compchemeng.2005.02.036.

Van Essen, G.M., Zandvliet, M.J., Van den Hof, P.M.J., Bosgra, O.H., and Jansen, J.D. (2006). Robust waterflooding optimization of multiple geological scenarios. In *SPE Annual Technical Conference and Exhibition*. San Antonio, Texas, U.S.A. doi:10.2118/102913-MS. SPE 102913-MS.